Convective–reactive nucleosynthesis of K, Sc, Cl and p-process isotopes in O–C shell mergers

C. Ritter,[1,2,3]★ R. Andrassy,[1,2] B. Côté,[1,2,3,4] F. Herwig,[1,2,3]★ P. R. Woodward,[2,5] M. Pignatari[3,6] and S. Jones[3,7]

[1]*Department of Physics and Astronomy, University of Victoria, Victoria, BC V8P5C2, Canada*
[2]*JINA-CEE, Michigan State University, East Lansing, MI 48823, USA*
[3]*NuGrid Collaboration (http://www.nugridstars.org)*
[4]*National Superconducting Cyclotron Laboratory, Michigan State University, MI 48823, USA*
[5]*LCSE and Department of Astronomy, University of Minnesota, Minneapolis, MN 55455, USA*
[6]*E. A. Milne Centre for Astrophysics, Department of Physics and Mathematics, University of Hull, Hull, HU6 7RX, UK*
[7]*Heidelberg Institute for Theoretical Studies, Schloss-Wolfsbrunnenweg 35, D-69118 Heidelberg, Germany*

ABSTRACT

We address the deficiency of odd-Z elements P, Cl, K and Sc in Galactic chemical evolution models through an investigation of the nucleosynthesis of interacting convective O and C shells in massive stars. 3D hydrodynamic simulations of O-shell convection with moderate C-ingestion rates show no dramatic deviation from spherical symmetry. We derive a spherically averaged diffusion coefficient for 1D nucleosynthesis simulations, which show that such convective–reactive ingestion events can be a production site for P, Cl, K and Sc. An entrainment rate of $10^{-3}\,\mathrm{M_\odot\,s^{-1}}$ features overproduction factors $\mathrm{OP_s} \approx 7$. Full O–C shell mergers in our 1D stellar evolution massive star models have overproduction factors $\mathrm{OP_m} > 1$ dex but for such cases 3D hydrodynamic simulations suggest deviations from spherical symmetry. γ-process species can be produced with overproduction factors of $\mathrm{OP_m} > 1$ dex, for example, for $^{130,\,132}$Ba. Using the uncertain prediction of the $15\,\mathrm{M_\odot}$, $Z = 0.02$ massive star model ($\mathrm{OP_m} \approx 15$) as representative for merger or entrainment convective–reactive events involving O- and C-burning shells, and assume that such events occur in more than 50 per cent of all stars, our chemical evolution models reproduce the observed Galactic trends of the odd-Z elements.

Key words: stars: abundances – stars: evolution – stars: interiors – physical data and processes: hydrodynamics – Galaxy: abundances.

1 INTRODUCTION

Massive stars are the main producers of intermediate-mass elements below the Fe peak (e.g. Woosley, Heger & Weaver 2002). However, the odd-Z elements K and Sc in Galactic chemical evolution (GCE) models of the Milky Way based on yields of Kobayashi et al. (2006, K06) or Nomoto, Kobayashi & Tominaga (2013) are up to 1 dex lower compared to halo and disc stars. Several promising production scenarios have been considered for Sc, such as the ejecta of proton-rich neutrino winds (Fröhlich et al. 2006), jet-induced core-collapse supernova explosions (e.g. Tominaga 2009) and hypernovae (e.g. Sneden et al. 2016). However, the impact of these mechanisms on GCE models has not yet been demonstrated. Massive stars are also considered the main source of rare p-rich stable isotopes beyond iron, although the underproduction

in simulations compared to the solar abundances has always been recognized (see Pignatari et al. 2016a, and references therein). Previous attempts to explain the production of odd-Z elements focused on explosive nucleosynthesis environments. We are proposing that odd-Z elements, as well as possibly p-process species, are forming in convective–reactive events in pre-supernova stellar evolution. In 1D stellar models, the mixing-length theory (Cox & Giuli 1968) describes convection in a time and spatially averaged way that provides realistic results when the Damköhler number $Da = \tau_{\mathrm{mix}}/\tau_{\mathrm{reac}} \ll 1$. Then, the convective region is instantaneously mixed and the detailed shape of the mixing profile is not important. However, in convective–reactive nucleosynthesis $Da \sim 1$ and the interaction of the mixing and nuclear processes determines the nucleosynthesis. In more extreme cases, the energy feedback from nuclear reactions on the convective turnover time-scale may be dynamically relevant, such as in H–ingestion into He-shell flash convection in post-AGB stars. This can lead to a 3D non-radial instability Global Oscillation of Shell H-ingestion (GOSH; Herwig et al. 2014). This

★ E-mail: critter@uvic.ca (CR); fherwig@uvic.ca (FH)

Table 1. Overview of simulations and their properties. Given are the entrainment rates $\dot{M}_e$, time-averaged O- and C-burning luminosities L_O and L_C and the increase of the Q values of O-shell by a factor fQO. [CR: C-shell fluid burning was increased by a factor fQC = 10 in I11. In contrast to I2 and I13 entrainment in I11 cannot be considered stationary anymore.] The luminosities of I13 and I11 vary in the time interval adopted for averaging by up to a factor of $\sim$4. The entrainment rate in I11 was derived using a different method to be described in Andrassy et al. (in preparation) and corresponds to the last 2.5 min before the flow became so violent that the simulation had to be stopped. Stellar evolution tracks of R17 with mean overproduction factors of convective O–C shell mergers $\overline{\text{OP}}$ of P, Cl, P and Sc, the increase of the diffusion coefficient by a factor f_D and the total run time t_{tot}. M_{ini} and Z are the initial mass and metallicity of the stellar evolution models.

Run ID	Hydrodynamic simulations			
	$\dot{M}_e$ (M$_\odot$ s^{-1})	L_O (L$_\odot$)	L_C (L$_\odot$)	f_{QO}
I2	3.13×10^{-7}	4.27×10^{10}	8.29×10^{9}	1.0
I13	1.07×10^{-4}	5.10×10^{12}	2.54×10^{12}	67.5
I11	2.24×10^{-4}	8.02×10^{11}	1.32×10^{13}	13.5
Run ID	1D post-processing simulations of I2			
	$\dot{M}_e$ (M$_\odot$ s^{-1})	$\overline{\text{OP}}_s$	f_D	t_{tot} (min)
Sm5	1.2×10^{-5}	1.23	1.0	16.5
Sm5L	1.2×10^{-5}	1.65	1.0	291.7
Sm4	1.2×10^{-4}	2.38	1.0	16.5
Sm3	1.2×10^{-3}	4.70	1.0	16.5
Sm3D	1.2×10^{-3}	7.00	15.7	16.5
Run ID	Stellar evolution tracks			
	$\overline{\text{OP}}_m$	M_{ini} (M$_\odot$)	Z	Reference
M15Z0.02	14.74	15	0.02	R17
M12Z0.01	8.34	12	0.01	R17
M15Z0.01	33.53	15	0.01	R17
M20Z0.01	12.15	20	0.01	R17
M25Z0.02R		20	0.02	R17
M25Z0.02J		25	0.02	J17

convective–reactive environment gives rise to exotic i-process nucleosynthesis (Herwig et al. 2011; Denissenkov et al. 2017).

2D hydrodynamic simulations of Meakin & Arnett (2006) suggested that the entrainment at the top of the O shell in a simultaneous O- and C-shell convection simulation can reach 10^{-4} M$_\odot$ s^{-1} and significantly affect the evolution. Nucleosynthesis in 1D models of O–C shell mergers has been mentioned in the literature (Rauscher et al. 2002; Tur, Heger & Austin 2007). In the NuGrid model library (Ritter et al. 2017, hereafter R17), O–C shell mergers are found in stellar models with initial mass between 12 and 20 M$_\odot$ at Z = 0.02 and 0.01 (Table 1).

We explore C ingestion into a convective O-shell with 3D hydrodynamic simulations. A diffusion coefficient profile is derived and applied in 1D nucleosynthesis simulations. Shell mergers in stellar evolution models are analysed and predictions tested against observations using GCE models. The simulation tools are introduced in Section 2, the results are in Section 3 and discussion and conclusion in Section 4.

2 METHODS

We perform 3D simulations of the first convective O shell as in Jones et al. (2017, hereafter J17). We adopt the same radial stratification based on a 25 M$_\odot$ stellar evolution model (M25Z0.02J, Table 1) and the same numerical approach (3D hydrodynamics code PPMstar, Woodward, Herwig & Lin 2015). We run simulations in 4π geometry on a 768^3 grid of the ingestion of C-rich material from a stable layer atop the O shell. We use a realistic O burning prescription according to Eq. 18.75 in Kippenhahn, Weigert & Weiss (2012).

Our initial nucleosynthesis analysis of C-shell material ingestion into the O shell with a 1-zone simulation showed that the ^{12}C(^{12}C, α)^{20}Ne (Caughlan & Fowler 1988) and the ^{16}O(α, g)^{20}Ne reactions produce most of the energy over most of the O shell. We assume that each α particle liberated by the first reaction immediately triggers the second since plenty of ^{16}O is available. Thus, the energy release of C burning is the sum of Q values of the two reactions. The mass fraction of ^{12}C in the C shell of the stellar model M25Z0.02J is 0.026. We use five times that value for the fluid in the top stable layer in this PPMstar simulation (I2) to shorten the transition to a stationary state. We perform additional runs with enhanced O- and C-burning energy release (Table 1).

The ^{16}O + ^{12}C reaction, which we ignore in this initial set of hydro simulations, may also become relevant, sensitively depending on the temperature, the mixing efficiency and the amount of entrained C-shell material. Indeed, in the I2 (I13) hydro simulations the C-shell fluid is mixed fast to the hottest layers in quantities such that the reaction provides a factor of 8 (0.7) more energy than the reactions included in the hydro network. A detailed analysis of this complex, non-linear problem is beyond the scope of this work and will be addressed elsewhere (Andrassy et al., in preparation).

The detailed nucleosynthesis is computed with the 1D multizone post-processing code MPPNP, as in Herwig et al. (2011). The stratification is the same as in the hydrodynamic simulation I2, which is based on the stellar model M25Z0.02J. C-shell material with an abundance distribution of the post-processed stellar model M25Z0.02R at a range of rates is injected into the upper part of the convective shell. Mixing is modelled based on a diffusion coefficient determined from the 3D simulations I2 (Fig. 2).

We model the chemical evolution of the Milky Way with a one-zone, open-box model with Galactic inflows and outflows in OMEGA (Côté et al. 2016, 2017), which is part of the NuGrid chemical evolution framework (Ritter & Côté 2016). Here, we use yields of AGB and massive star models from NuGrid (Pignatari et al. 2016b; R17) and, alternatively, of massive stars from K06, as well as of Population III stars (Heger & Woosley 2010) and SNeIa (Seitenzahl et al. 2013). The initial mass function of Kroupa (2001) is adopted over the initial mass range from 0.1 to $100 \, M_\odot$, and we assume the ejection of stellar yields between the initial masses of 1 and $30 \, M_\odot$.

3 RESULTS

3.1 Convection and feedback in 3D

3D hydrodynamic simulations of J17 of the first O shell show a mass entrainment rate of $1.3 \times 10^{-6} \, M_\odot \, s^{-1}$. If the O shell of that underlying stellar model grows outwards at this rate, then it can reach the C shell in $1.9 \, d$. This is before the end of O-shell convection, which suggests the possibility of significantly enhanced entrainment rates or even an O–C shell merger.

In simulation I2, C-rich material is entrained into the O shell over 110 convective turnover times of $132 \, s$. The burning of the entrained material is turned off in the code for the first 34 turnovers. The entrained fluid reaches the bottom of the convective O shell (Fig. 1) and, after C burning has been turned on, its spherically averaged abundance develops towards a stationary state with an entrainment rate of $3.13 \times 10^{-7} \, M_\odot \, s^{-1}$. This rate is lower than that measured by J17 because (1) the luminosity is lower in our case, and (2) our experience to date with the PPMstarcode's present version indicates a decline in ingestion rate at very low luminosities that falls below well-established trends that we observe at higher luminosities. We suspect this fall-off to be due to numerical rather than physical causes at the grid resolution of run I2, namely 768^3 cells. Checking that the ingestion rate has converged using simulations of double the grid resolution of run I2 is quite expensive, and such checks have been successfully carried out already for high-luminosity cases (cf. J17). We are addressing this issue instead by modifying the code to compute in future a potentially fully non-linear perturbation to the star's very rapidly varying base state.

The energy release from C burning does not significantly affect the flow properties in I2. The stationary nature and approximate spherical symmetry of the convective shell justify approximating the 3D mixing with a diffusion coefficient (see J17 for details) and applying it in 1D nucleosynthesis models.

Significantly higher ingestion rates might occur when the O-shell merges with the C-shell, or in a later and more luminous pre-supernova O shell (J17, Meakin & Arnett 2006). For this phase, the 1D stellar models of R17 do show in fact O–C shell mergers for several cases (Table 1). In order to start exploring 3D hydrodynamic properties of such high-entrainment or even merger regimes, we artificially increase the O-burning luminosity in simulation I13 by ≈ 2 dex to $5.1 \times 10^{12} \, L_\odot$ by increasing the Q value of the O-burning reaction by a factor of 67.5, which corresponds to the increase between the first and second O shell of the stellar model M15Z0.02 (Table 1). The average entrainment rate is $1.07 \times 10^{-4} \, M_\odot \, s^{-1}$ in this case, in agreement with the entrainment-luminosity law of J17. The flow is more inhomogeneous and the convective boundary is significantly more deformed than in I2 (Fig. 1), but we do not find any global entrainment instability (cf. Herwig et al. 2014). Therefore, at this high entrainment rate nucleosyn-
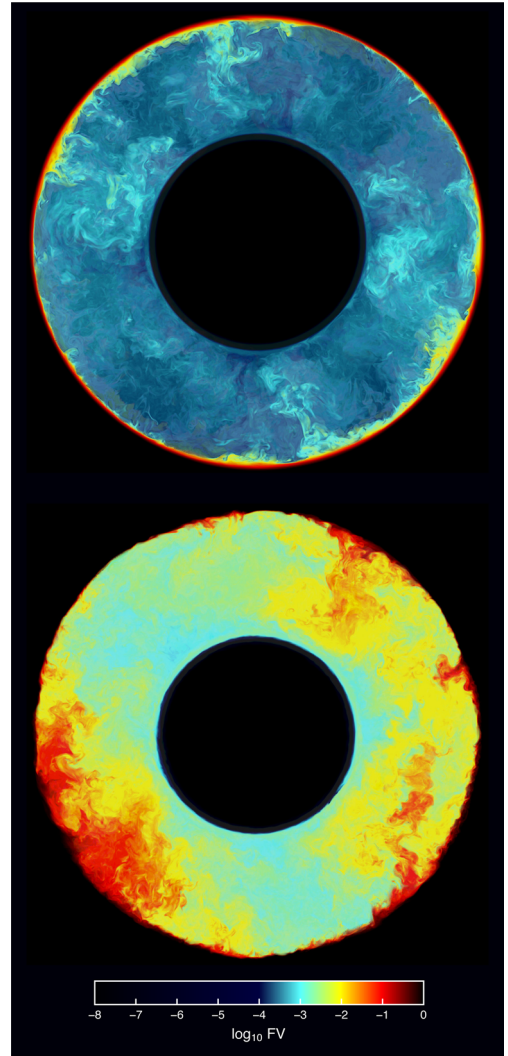
Figure 1. Volume fraction of the C-rich fluid in a sphere slice of 3D convective O-shell simulations on a 768^3 grid. Top panel: Simulation I2 after $148 \, min$. Bottom panel: Run I13 after $10.5 \, min$. The entrainment rate is 342 times higher than in I2.

thesis may still be estimated from spherically symmetric MPPNP simulations.

The mass exchange in shell mergers could initially be hindered by the entropy gradient between the shells However, strong non-spherical instabilities similar to the GOSH can occur with an unknown range of effective C-burning luminosities. In order to explore such scenarios, we perform as an experiment simulation I11 (Table 1) were we enhance the energy release from O and C burning fluid by factors of 13.5 and 10.0, respectively. In this case a violent, global, non-radial oscillation does emerge.

3.2 Nucleosynthesis in 1D

We perfom 1D MPPNP simulations for a range of ingestion rates (Table 1), from 1.2×10^{-7} to $1.2 \times 10^{-3} \, M_\odot \, s^{-1}$, at which point the whole C shell would be entrained in $1000 \, s$, which is approximately eight overturning time-scales. In the limit of near-sonic mass transport, the mass exchange rate could even reach $1 \, M_\odot \, s^{-1}$.

With entrainment rates corresponding to hydro run I2 no relevant production of odd-Z elements is observed. For an entrainment rate of
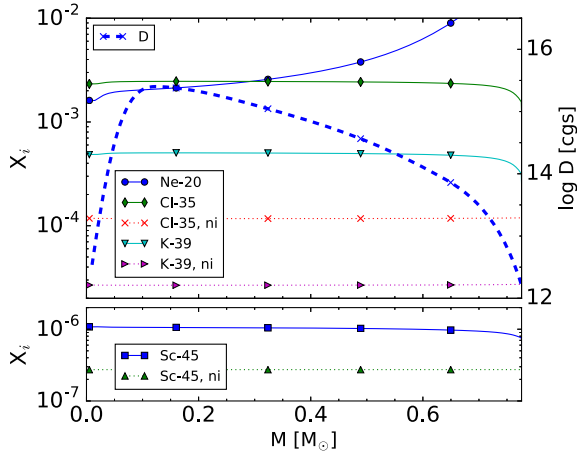
Figure 2. Abundance profiles of run Sm4 after 16.5 min of ingesting C-shell material at a rate of $1.2 \times 10^{-4} M_\odot s^{-1}$. For comparison, the abundances produced over the same time with no ingestion (ni). The diffusion coefficient D is extracted from the 3D hydrodynamic simulation I2.
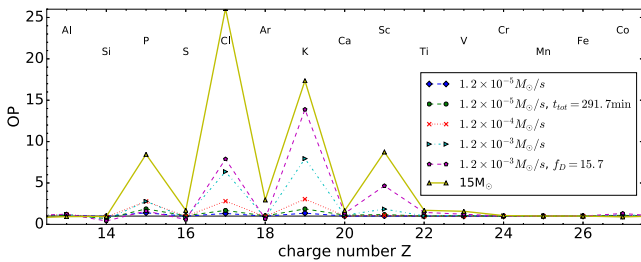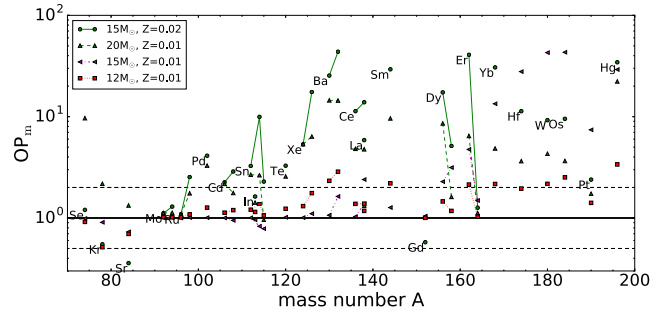

Figure 3. Overproduction factors OP_s due to C-shell ingestion for different entrainment rates of C-shell material, total run times and diffusion coefficients in our synthetic models (Table 1). In comparison the overproduction factors OP_m in the O–C shell merger of the stellar model M15Z0.02.

$1.2 \times 10^{-5} M_\odot s^{-1}$ the O shell may reach the C shell in 291.7 min, without any significant element production (Sm5, Sm5L). For entrainment rates that correspond to 3D simulation I13 (MPPNP run Sm4, Table 1) and above, considerable amounts of ^{35}Cl, ^{39}K and ^{45}Sc (Fig. 2) as well as ^{31}P are produced in the lower part of the O shell through convective–reactive entrainment and burning of ^{20}Ne. The element production of Cl, K and Sc is larger for higher convective velocities and for higher entrainment rates (Table 1).

Through repeated multizone simulations with individual rates turned off it emerges that burning of ingested Ne leads to the production of odd-Z isotopes ^{31}P, ^{35}Cl, ^{39}K and ^{45}Sc at different depths in the convective zone. (γ,p) reactions, such as $^{31}P(\gamma,p)$, release protons that produce odd-Z elements through reactions such as $^{38}Ar(p,\gamma)^{39}K$. A further detailed investigation of this convective–reactive nucleosynthesis site is required to fully determine the nucleosynthesis paths that involve conditions at several layers simultaneously.

In order to consider properly contributions from all burning shells to the total stellar yields, we compare the material produced in an O-shell with ingestion (Y_i) to the material that would result without ingestion (Y_{ni}) relative to the total yields Y_{tot} of the stellar model M25Z0.02R (Fig. 3). Thus, the overproduction factor for 1D MPPNP runs is $OP_s = (Y_i + Y_{tot})/(Y_{ni} + Y_{tot})$.

The 1D stellar model M15Z0.02 experiences an O–C shell merger about 4 min after the end of convective Si core burning. After an initial partial mixing phase both convective shells merge, and large

Figure 4. Overproduction factors OP_m of p nuclei in O–C shell mergers of stellar models of NuGrid. ^{180}Ta values are omitted for clarity and are 2.95, 0.7, 5.61 and 0.64 in legend order, starting from the top. The dashed horizontal lines show an overproduction factor of 0.5 and 2.

amounts of ^{35}Cl, ^{39}K and ^{45}Sc are produced (Fig. 3). Again, the 1D simulations are not reliable at such high entrainment rates, but merely indicative (see Section 3.1). For stellar models the overproduction factors are calculated as $OP_m = Y_f/Y_{ini}$, where Y_{ini} and Y_f are the total amounts of material above the mass cut at onset and after inter-shell mixing, respectively (Table 1). Fallback is taken into account with the adoption of the mass cut of the delayed explosion prescription, as in R17. The overproduction factors due to the O–C shell merger in the stellar model are qualitatively similar to what we found in our 1D MPPNP ingestion simulations (Fig. 3).

The O shell is significantly modified by the core-collapse SN explosion and affected by fallback. We use the core-collapse supernova (CCSN) prescription for the stellar model M15Z0.02 with a neutron-star remnant coordinate based on the delayed explosion prescription of Fryer et al. (2012). The remnant coordinate is below the peak production of ^{31}P, ^{35}Cl, ^{39}K and ^{45}Sc. The overproduction factors based on the explosive nucleosynthesis indicate that P, Cl, K and Sc are little affected in our explosion model.

The γ process occurs in Ne and O shell burning in the CCSN explosion of massive star models through photodisintegration reactions on heavy elements (Woosley & Howard 1978; Pignatari et al. 2016a). During an O–C shell merger, 'fresh' heavy elements are constantly transported down into the O-burning shell, providing new seeds for photodisintegration.

We compare the overproduction factors of the classical 35 p nuclei of the O–C shell merger in the stellar models M15Z0.02, M20Z0.01, M15Z0.01 and M12Z0.01 (Fig. 4). In these models, we find strong variations in the overproduction factors with stellar mass and metallicity. Light p nuclei are destroyed while heavier species are effectively produced. Most of those species have the largest overproduction factors in the stellar model M15Z0.02. We confirm the results of Rauscher et al. (2002) that p nuclei can be made in an O–C shell merger. At this level of production, the impact of O–C shell mergers may change the GCE scenario of at least some of the p nuclei.

3.3 K and Sc trends in the milky way

Some stellar models of R17 at $Z = 0.01$ and 0.02 show O–C shell mergers (Table 1). These shell mergers cause the rise in [K, Sc/Fe] above [Fe/H] > −1 with NuGrid yields in Fig. 5. We infer that the K06 and Nomoto et al. (2013) yields do not have significant O–C shell mergers.

We explore the assumption that shell mergers can happen in all massing star models at all Z by applying the material produced in the O–C shell merger of model M15Z0.02 to all massive star models
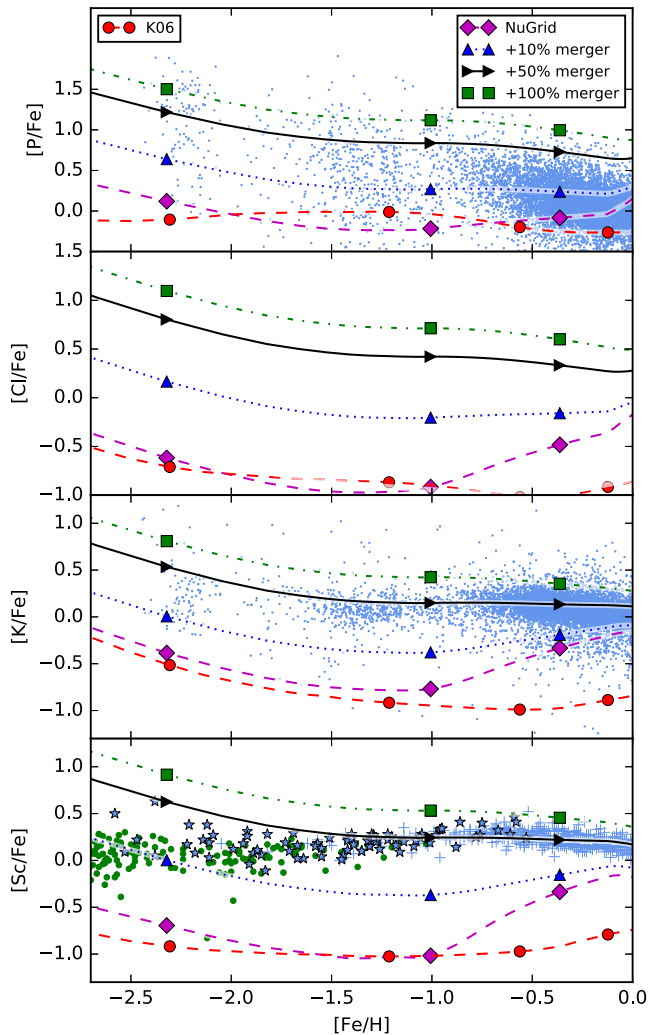
Figure 5. Comparison of the predictions of P, Cl, K and Sc of our Milky Way model with observational data (if available). Predictions with 10 per cent, 50 per cent and 100 per cent addition of material produced in the O–C shell merger of the stellar model M15Z0.02 to all massive stars without O–C shell merger. For comparison, we show GCE predictions based on yields from K06. P and K data are from the APOGEE survey (Albareti et al. 2016), and Sc data from Ishigaki, Chiba & Aoki (2012, 2013, crosses); Roederer et al. (2014, dots) and Battistini & Bensby (2015, stars).

which do not experience O–C shell mergers. We add the material to a fraction of 10 per cent, 50 per cent and 100 per cent of these stars. If the merger fraction defined in this way is between 10 per cent and 50 per cent the observed amounts of K and Sc can be reproduced (Fig. 5).

An increased γ-process production via O–C shell mergers might also boost the Galactic γ-process contribution of massive stars. In Rayet et al. (1995), a global underproduction of p nuclides in massive stars compared to what is necessary to explain the Solar system distribution is found. We speculate that the shell merger production could enable us to match the solar distribution when assuming a wide spectrum of entrainment rates, 3D hydrodynamic merger conditions and stellar structures.

4 DISCUSSION AND CONCLUSION

Our results have a number of limitations. In our GCE model test, we add material produced in one particular O–C shell merger from a

1D stellar evolution model. The 1D model prediction are uncertain because 3D effects will likely play an important role. In addition, we neglect the dependence on initial mass and metallicity. While more massive stars are affected by larger fallback (Fryer et al. 2012), they also inhibit larger O and C shells that boost the γ-process production. A larger convective C shell enables the entrainment of more material, which boosts the production of elements such as P, Cl and K, can be transported further outwards and will be less affected by fallback. The time-span between the onset of an O–C shell merger and core collapse is also crucial to enable sufficient element production.

Higher temperatures in the O shells of lower mass stars might lead to a stronger production of lighter p nuclei, which are transported into the upper part of the C shell. For the highest masses, such as the 25 M$_\odot$ R17 models at all metallicities, the C-shell convection is either patchy or absent (especially at lower Z), which may help or hinder ingestion of C-shell material.

More generally, stellar evolution models indicate that O–C shell mergers may happen. In some cases they do, in others the shells are just stopping short of a merger, depending on various uncertain modeling assumptions in 1D. But even if the stellar evolution uncertainties are addressed to the best of our ability the question of whether a merger will happen in a particular, possibly marginal, case requires sufficiently realistic 3D hydrodynamic simulations. Once it is clear under which conditions O–C shell mergers happen, 3D simulations will be required to determine how O–C shell mergers proceed, whether they are ultimately dominated by non-radial, global oscillations, and how the nuclear burning energy feedback alters the flow.

In our 3D hydrodynamic simulations, we observe approximately spherically symmetric, quasi-steady-state behaviour for entrainment rates that lead to noticeable odd-Z element production. To fully explain the lack of Sc and K in present yields for GCE models actual mergers of the O and C shells are required. Our preliminary 3D simulation experiments suggest that the assumption of spherical symmetry may break down for such conditions. GCE simulations that assume that O–C shell mergers as in model M15Z0.02 occur in $\approx$10 per cent to 50 per cent of all massive stars can account for the observed abundance of K and Sc in Milky Way stars.

Our 1D nucleosynthesis models so far display a wide range of ^{39}K/^{41}K and ^{35}Cl/^{37}Cl ratios, depending on mixing and thermodynamic details, some of them within a factor of a few and some much larger compared to the solar ratios. The isotopic ratios will be an important constraint for more realistic 3D models with updated nuclear physics.

With the entrainment of C-shell material heavy-element seeds are swept into the O shell and serve as a boost for the p-nuclei production. In 1D stellar models, we find a variety of production efficiencies which vary with initial mass and metallicity and the overproduction factors are more than 1 dex for many isotopes beyond Ba. Such strong production might influence the GCE of p-process isotopes. A future investigation will be required to test this scenario.

Canada were used. We acknowledge Brad Gibson for reminding us to check the isotopic ratios of our models.

REFERENCES

Albareti F. D. et al. 2016, preprint (arXiv:arXiv:e-prints)

Battistini C., Bensby T., 2015, VizieR Online Data Catalog, 357

Caughlan G. R., Fowler W. A., 1988, At. Data Nucl. Data Tables, 40, 283

Côté B., West C., Heger A., Ritter C., O'Shea B. W., Herwig F., Travaglio C., Bisterzo S., 2016, MNRAS, 463, 3755

Côté B., O'Shea B. W., Ritter C., Herwig F., Venn K. A., 2017, ApJ, 835, 128

Cox J. P., Giuli R. T., 1968, Principles of stellar structure. Gordon and Breach, New York

Denissenkov P. A., Herwig F., Battino U., Ritter C., Pignatari M., Jones S., Paxton B., 2017, ApJ, 834, L10

Fröhlich C. et al., 2006, ApJ, 637, 415

Fryer C. L., Belczynski K., Wiktorowicz G., Dominik M., Kalogera V., Holz D. E., 2012, ApJ, 749, 91

Heger A., Woosley S. E., 2010, ApJ, 724, 341

Herwig F., Pignatari M., Woodward P. R., Porter D. H., Rockefeller G., Fryer C. L., Bennett M., Hirschi R., 2011, ApJ, 727, 89

Herwig F., Woodward P. R., Lin P.-H., Knox M., Fryer C., 2014, ApJ, 792, L3

Ishigaki M. N., Chiba M., Aoki W., 2012, ApJ, 753, 64

Ishigaki M. N., Aoki W., Chiba M., 2013, ApJ, 771, 67

Jones S., Andrassy R., Sandalski S., Davis A., Woodward P., Herwig F., 2017, MNRAS, 465, 2991 (J17)

Kippenhahn R., Weigert A., Weiss A., 2012, Stellar Structure and Evolution, Springer-Verlag, Berlin, Heidelberg

Kobayashi C., Umeda H., Nomoto K., Tominaga N., Ohkubo T., 2006, ApJ, 653, 1145

Kroupa P., 2001, MNRAS, 322, 231

Meakin C. A., Arnett D., 2006, ApJ, 637, L53

Nomoto K., Kobayashi C., Tominaga N., 2013, ARA&A, 51, 457

Pignatari M., Göbel K., Reifarth R., Travaglio C., 2016a, Int. J. Mod. Phys. E, 25, 1630003

Pignatari M. et al., 2016b, ApJS, 225, 24

Rauscher T., Heger A., Hoffman R. D., Woosley S. E., 2002, ApJ, 576, 323

Rayet M., Arnould M., Hashimoto M., Prantzos N., Nomoto K., 1995, A&A, 298, 517

Ritter C., Côté B., 2016, NuPyCEE: NuGrid Python Chemical Evolution Environment, Astrophysics Source Code Library

Ritter C., Herwig F., Jones S., Pignatari M., Fryer C., Hirschi R., 2017, MNRAS, preprint (arXiv:1709.08677) (R17)

Roederer I. U., Preston G. W., Thompson I. B., Shectman S. A., Sneden C., Burley G. S., Kelson D. D., 2014, AJ, 147, 136

Seitenzahl I. R. et al., 2013, MNRAS, 429, 1156

Sneden C., Cowan J. J., Kobayashi C., Pignatari M., Lawler J. E., Den Hartog E. A., Wood M. P., 2016, ApJ, 817, 53

Tominaga N., 2009, ApJ, 690, 526

Tur C., Heger A., Austin S. M., 2007, ApJ, 671, 821

Woodward P. R., Herwig F., Lin P.-H., 2015, ApJ, 798, 49

Woosley S. E., Howard W. M., 1978, ApJS, 36, 285

Woosley S. E., Heger A., Weaver T. A., 2002, Rev. Mod. Phys., 74, 1015

This paper has been typeset from a TEX/LATEX file prepared by the author.